

Higgs-pair Production and Decay in Simplest Little Higgs Model

Xiao-Fang Han¹, Lei Wang^{2,*}, Jin Min Yang¹

¹ *Key Laboratory of Frontiers in Theoretical Physics,
Institute of Theoretical Physics, Academia Sinica, Beijing 100190, China*

² *Department of Physics, Yantai University, Yantai 264005, China*

Abstract

In the framework of the simplest little Higgs model (SLHM), we study the production of a pair of neutral CP-even Higgs bosons at the LHC. First, we examine the production rate and find that it can be significantly larger than the SM prediction. Then we investigate the decays of the Higgs-pair and find that for a low Higgs mass their dominant decay mode is $hh \rightarrow \eta\eta\eta\eta$ (η is a CP-odd scalar) while $hh \rightarrow b\bar{b}\eta\eta$ and $hh \rightarrow \eta\eta WW$ may also have sizable ratios. Finally, we comparatively study the rates of $pp \rightarrow hh \rightarrow b\bar{b}\tau^+\tau^-$, $pp \rightarrow hh \rightarrow b\bar{b}\gamma\gamma$, and $pp \rightarrow hh \rightarrow WWWW$ in the SLHM and the littlest Higgs models (LHT). We find that for a light Higgs, compared with the SM predictions, all the three rates can be sizably enhanced in the LHT but severely suppressed in the SLHM; while for an intermediately heavy Higgs, both the LHT and SLHM can enhance sizably the SM predictions.

PACS numbers: 14.80.Cp, 12.60.Fr, 11.30.Qc

* Corresponding author. Email address: leiwang@itp.ac.cn (L. Wang)

I. INTRODUCTION

Little Higgs theory [1] has been proposed as an interesting solution to the hierarchy problem. So far various realizations of the little Higgs symmetry structure have been proposed [2, 3, 4, 5], which can be categorized generally into two classes [6]. One class use the product group, represented by the littlest Higgs model [4], in which the SM $SU(2)_L$ gauge group is from the diagonal breaking of two (or more) gauge groups. The other class use the simple group, represented by the simplest little Higgs model (SLHM) [5], in which a single larger gauge group is broken down to the SM $SU(2)_L$. Of course, different realizations give different phenomenology, which will be tested at the LHC

Since these little Higgs models mainly alter the properties of the Higgs boson and the top quark, hints of these models may be unravelled from various Higgs boson and top quark processes [7]. The Higgs-pair production at the LHC, albeit with a small production rate, is rather important because it will provide a way to probe the Higgs self-coupling λ . With the designed luminosity, it is possible for the LHC to establish that the SM Higgs boson has a non-zero self-coupling and the ratio λ/λ_{SM} can be restricted to a range of $0 - 3.7$ at 95% confidence level if its mass is between 150 GeV and 200 GeV [8]. Such Higgs-pair production is sensitive to new physics and has been studied in various new physics models [9]. In the littlest Higgs models without and with T-parity, this process was studied in [10] and [11], respectively. In this work, we study this process in the SLHM. We will first examine the Higgs-pair production rate in the SLHM and compare with the SM prediction. Then we study the decays of the Higgs-pair. Finally, we study the rates of $pp \rightarrow hh \rightarrow b\bar{b}\tau^+\tau^-$ ($b\bar{b}\gamma\gamma$) and $pp \rightarrow hh \rightarrow WWWW$, comparing the prediction of the SLHM with the littlest Higgs models.

This work is organized as follows. In Sec. II we recapitulate the SLHM. In Sec. III we calculate the Higgs-pair production cross section at the LHC. In Sec. IV, we study the decays of the Higgs-pair and the rates of $pp \rightarrow hh \rightarrow b\bar{b}\tau^+\tau^-$ ($b\bar{b}\gamma\gamma$) and $pp \rightarrow hh \rightarrow WWWW$. Finally, we give our conclusion in Sec. V.

II. SIMPLEST LITTLE HIGGS MODEL

The SLHM is based on $[SU(3) \times U(1)_X]^2$ global symmetry. The gauge symmetry $SU(3) \times U(1)_X$ is broken down to the SM electroweak gauge group by two copies of scalar fields Φ_1 and Φ_2 , which are triplets under the $SU(3)$ with aligned VEVs f_1 and f_2 . The uneaten five pseudo-Goldstone bosons can be parameterized as

$$\Phi_1 = e^{i t_\beta \Theta} \begin{pmatrix} 0 \\ 0 \\ f_1 \end{pmatrix}, \quad \Phi_2 = e^{-i t_\beta \Theta} \begin{pmatrix} 0 \\ 0 \\ f_2 \end{pmatrix}, \quad (1)$$

where

$$\Theta = \frac{1}{f} \left[\begin{pmatrix} 0 & 0 & H \\ 0 & 0 & \\ H^\dagger & 0 & \end{pmatrix} + \frac{\eta}{\sqrt{2}} \begin{pmatrix} 1 & 0 & 0 \\ 0 & 1 & 0 \\ 0 & 0 & 1 \end{pmatrix} \right], \quad (2)$$

$f = \sqrt{f_1^2 + f_2^2}$ and $t_\beta \equiv \tan\beta = f_2/f_1$. Under the $SU(2)_L$ SM gauge group, η is CP-odd singlet, while H transforms as a doublet and can be identified as the SM Higgs doublet. The kinetic term in the non-linear sigma model is

$$\mathcal{L}_\Phi = \sum_{j=1,2} \left| \left(\partial_\mu + ig A_\mu^a T^a - i \frac{g_x}{3} B_\mu^x \right) \Phi_j \right|^2, \quad (3)$$

where $g_x = g \tan\theta_W / \sqrt{1 - \tan^2\theta_W/3}$ with θ_W being the electroweak mixing angle. As Φ_1 and Φ_2 develop their VEVs, the new heavy gauge bosons Z' , Y^0 , and W'^{\pm} get their masses proportional to f .

The gauged $SU(3)$ symmetry promotes the SM fermion doublets into $SU(3)$ triplets. There are two possible gauge charge assignments for the fermions: the 'universal' embedding and the 'anomaly-free' embedding. The first choice is not favored by the electroweak precision data [5], so we focus on the second way of embedding. The quark Yukawa interactions for the third generation and the first two generations can be written respectively as

$$\mathcal{L}_3 = i\lambda_1^t t_1^c \Phi_1^\dagger Q_3 + i\lambda_2^t t_2^c \Phi_2^\dagger Q_3 + i \frac{\lambda_d^m}{\Lambda} d_m^c \epsilon_{ijk} \Phi_1^i \Phi_2^j Q_3^k + h.c., \quad (4)$$

$$\mathcal{L}_{1,2} = i\lambda_1^{d_n} d_{1n}^c Q_n^T \Phi_1 + i\lambda_2^{d_n} d_{2n}^c Q_n^T \Phi_2 + i \frac{\lambda_u^{mn}}{\Lambda} u_m^c \epsilon_{ijk} \Phi_1^{*i} \Phi_2^{*j} Q_n^k + h.c., \quad (5)$$

where $n = 1, 2$ are the first two generations indices; $i, j, k = 1, 2, 3$; $Q_3 = \{t_L, b_L, iT_L\}$ and $Q_n = \{d_{nL}, -u_{nL}, iD_{nL}\}$; d_m^c runs over $(d^c, s^c, b^c, D^c, S^c)$; d_{1n}^c and d_{2n}^c are linear combinations of d^c and D^c for $n = 1$ and of s^c and S^c for $n = 2$; u_m^c runs over (u^c, c^c, t^c, T^c) . For simplicity, we assume the quark flavor mixing are small and neglect the mixing effects. From Eqs. (4) and (5), we can get the Higgs boson interactions and the mass terms for the three generations of quarks:

$$\mathcal{L}_t \simeq -f\lambda_2^t [x_\lambda^t c_\beta t_1^c (-s_1 t_L + c_1 T_L) + s_\beta t_2^c (s_2 t_L + c_2 T_L)] + h.c., \quad (6)$$

$$\mathcal{L}_{d_n} \simeq -f\lambda_2^{d_n} [x_\lambda^{d_n} c_\beta d_1^c (s_1 d_{nL} + c_1 D_{nL}) + s_\beta d_2^c (-s_2 d_{nL} + c_2 D_{nL})] + h.c., \quad (7)$$

$$\mathcal{L}_q \simeq -\frac{\lambda_q}{\Lambda} f^2 s_\beta c_\beta s_3 q^c q_L + h.c. \quad (q = u, c, b) \quad (8)$$

where

$$\begin{aligned} x_\lambda^t &\equiv \frac{\lambda_1^t}{\lambda_2^t}, & x_\lambda^{d_n} &\equiv \frac{\lambda_1^{d_n}}{\lambda_2^{d_n}}, & s_\beta &\equiv \frac{f_2}{\sqrt{f_1^2 + f_2^2}}, & c_\beta &\equiv \frac{f_1}{\sqrt{f_1^2 + f_2^2}}, \\ s_1 &\equiv \sin \frac{t_\beta (h+v)}{\sqrt{2}f}, & s_2 &\equiv \sin \frac{(h+v)}{\sqrt{2}t_\beta f}, & s_3 &\equiv \sin \frac{(h+v)(t_\beta^2 + 1)}{\sqrt{2}t_\beta f}, \end{aligned} \quad (9)$$

with h and v being the neutral Higgs boson field and its VEV, respectively. The mass eigenstates are obtained by mixing the corresponding interaction eigenstates, e.g., the mass eigenstates (t_{mL}, T_{mL}) and (t_m^c, T_m^c) are respectively the mixtures of (t_L, T_L) and (t^c, T^c) . The diagonalization of the mass matrix in Eqs.(6) and (7) was performed numerically in our analysis, and the relevant couplings with Higgs boson can also be obtained without resort to any expansion of v/f . Hereafter we denote the mass eigenstates without the subscript 'm' for simplicity.

The Yukawa and gauge interactions break the global symmetry and then provide a potential for the Higgs boson. However, the Coleman-Weinberg potential alone is not sufficient since the generated Higgs mass is too heavy and the new CP-odd scalar η is massless. Therefore, one can introduce a tree-level μ term which can partially cancel the Higgs mass [5, 12]:

$$-\mu^2(\Phi_1^\dagger \Phi_2 + h.c.) = -2\mu^2 f^2 s_\beta c_\beta \cos\left(\frac{\eta}{\sqrt{2}s_\beta c_\beta f}\right) \cos\left(\frac{\sqrt{H^\dagger H}}{f c_\beta s_\beta}\right). \quad (10)$$

The scalar potential becomes

$$V = -m^2 H^\dagger H + \lambda(H^\dagger H)^2 - \frac{1}{2}m_\eta^2 \eta^2 + \lambda' H^\dagger H \eta^2 + \dots, \quad (11)$$

where

$$m^2 = m_0^2 - \frac{\mu^2}{s_\beta c_\beta}, \quad \lambda = \lambda_0 - \frac{\mu^2}{12s_\beta^3 c_\beta^3 f^2}, \quad \lambda' = -\frac{\mu^2}{4f^2 s_\beta^3 c_\beta^3}, \quad (12)$$

with m_0 and λ_0 being respectively the one-loop contributions to the Higgs boson mass and the quartic couplings from the contributions of fermion loops and gauge boson loops [5].

The Higgs VEV, the Higgs boson mass and the mass of η are given by

$$v^2 = \frac{m^2}{\lambda}, \quad m_h^2 = 2m^2, \quad m_\eta^2 = \frac{\mu^2}{s_\beta c_\beta} \cos\left(\frac{v}{\sqrt{2}f s_\beta c_\beta}\right). \quad (13)$$

The Coleman-Weinberg potential involves the following parameters:

$$f, x_\lambda^t, t_\beta, \mu, m_\eta, m_h, v. \quad (14)$$

Due to the modification of the observed W gauge boson mass, v is defined as [12]

$$v \simeq v_0 \left[1 + \frac{v_0^2}{12f^2} \frac{t_\beta^4 - t_\beta^2 + 1}{t_\beta^2} - \frac{v_0^4}{180f^4} \frac{t_\beta^8 - t_\beta^6 + t_\beta^4 - t_\beta^2 + 1}{t_\beta^4} \right], \quad (15)$$

where $v_0 = 246$ GeV is the SM Higgs VEV. Assuming that there are no large direct contributions to the potential from physics at the cutoff, we can determine other parameters in Eq. (14) from f , t_β and m_h with the definition of v in Eq. (15).

III. HIGGS-PAIR PRODUCTION AT LHC

At the LHC the Higgs-pair production can proceed through gluon-gluon fusion and $b\bar{b}$ annihilation, as shown in Figs. (1) and (2), respectively. For the $b\bar{b}$ annihilation process, the SLHM can give the additional contributions through the tree-level $hhb\bar{b}$ coupling and the modified $hb\bar{b}$ coupling. For the gluon-gluon fusion process, the top-quark loops give additional contributions through the tree-level $hht\bar{t}$ coupling and the modified $ht\bar{t}$ coupling. In addition to the top-quark loops, the loops of the new heavy partner quarks T , D and S also come into play. Due to the large top quark Yukawa coupling and the large parton distribution function of gluon at the LHC, the contributions of the gluon-gluon fusion process can be dominant over $b\bar{b}$ annihilation process.

The calculations of the loop diagrams in Fig. 1 are straightforward. Each loop diagram is composed of some scalar loop functions [13] which are calculated by using LoopTools [14]. The calculations are tedious and the analytical expressions are lengthy, which are not

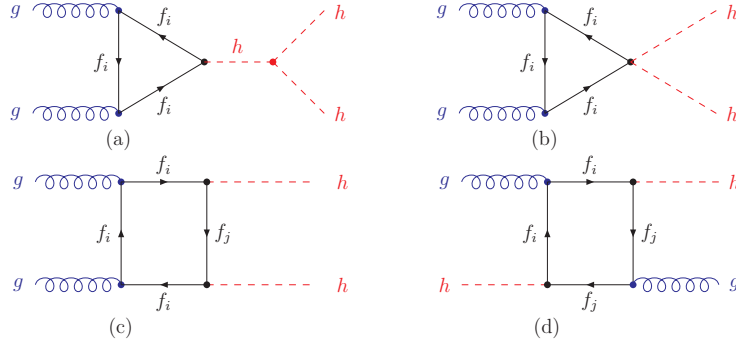


FIG. 1: Feynman diagrams for Higgs-pair production via gluon-gluon fusion in the SLHM. Here $i, j = 1, 2$ with (f_1, f_2) denoting (t, T) or (d, D) or (s, S) . The diagrams by exchanging the two gluons or exchanging the two Higgs bosons in (c,d) are not shown here.

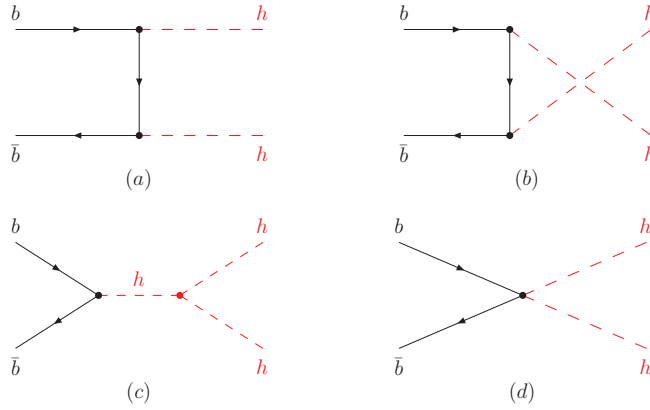


FIG. 2: Feynman diagrams for Higgs-pair production via $b\bar{b}$ annihilation in the SLHM.

presented here. The hadronic cross section at the LHC is obtained by convoluting the parton cross section with the parton distribution functions. In our calculations we use CTEQ6L [15] to generate the parton distributions with the renormalization scale μ_R and the factorization scale μ_F chosen to be $\mu_R = \mu_F = 2m_h$ and use the two-loop running coupling constant α_s with $\alpha_s(m_Z) = 0.118$.

The SM input parameters relevant in our study are taken as $m_t = 171.2$ GeV and $m_Z = 91.1876$ GeV [16]. The free SLHM parameters are $f, t_\beta, m_h, x_\lambda^d(m_D)$ and $x_\lambda^s(m_S)$. As shown above, the parameters x_λ^t, μ, m_η can be determined by f, t_β, m_h and v . The small mass of the d (s) quark requires one of the couplings λ_1^d and λ_2^d (λ_1^s and λ_2^s) to be very small, so there is almost no mixing between the SM down-type quarks and their heavy partners. We assume λ_1^d (λ_1^s) is small, and take $x_\lambda^d = 1.1 \times 10^{-4}$ and $x_\lambda^s = 2.1 \times 10^{-3}$, which can make the masses of D and S in the range of 1-2 TeV with other parameters fixed as in our

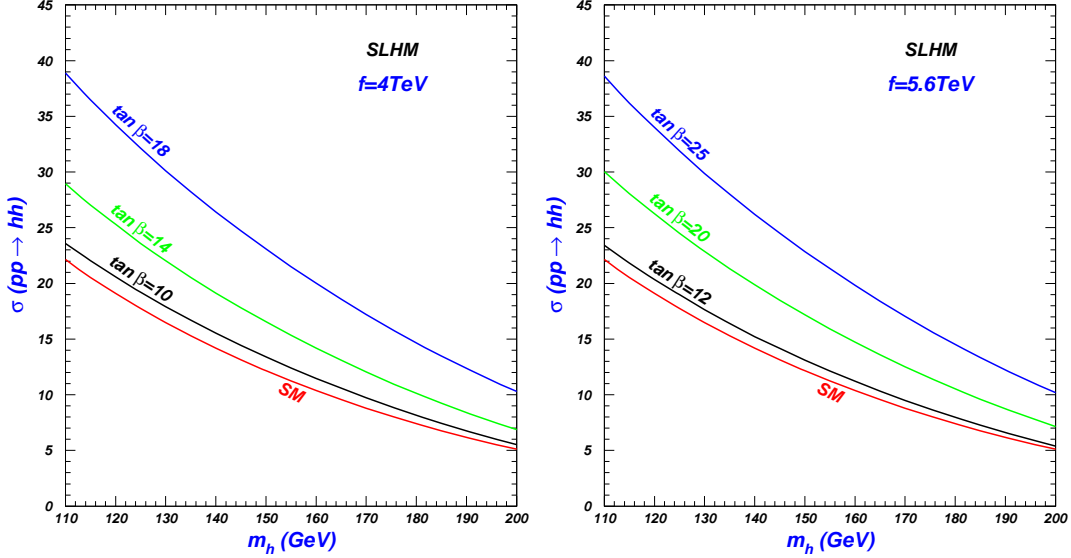


FIG. 3: Hadronic cross section of Higgs-pair production at the LHC versus the Higgs boson mass.

calculations. In fact, our results show that the contributions from d and D (s and S) are small compared with the effects from t and T . So, different choices of x_λ^d and x_λ^s do not have sizable effects on our results.

Electroweak precision data can give the strong constraints on the scale f . The [5] shows that the LEP-II data requires $f > 2$ TeV. In addition, the contributions to electroweak precision data can be suppressed by large t_β . Ref. [17] gives a lower bound of $f > 4.5$ TeV from the oblique parameter S while a recent study of Z leptonic decay gives a stronger bound of $f > 5.6$ TeV [18]. Considering the above bounds, we take $f = 4$ TeV or $f = 5.6$ TeV with a large $\tan\beta$ to illustrate our results.

In Fig. 3, we take several values of $\tan\beta$ and plot the hadronic cross section of Higgs-pair production at the LHC versus the Higgs boson mass. We find that compared with the SM prediction, the cross section in the SLHM can be significantly enhanced for a large $\tan\beta$. For example, with $\tan\beta=18$ (25) and $f = 4$ TeV (5.6 TeV), the cross section can be enhanced by 80% for $m_h = 110$ GeV. Of course, for the perturbation to be valid, $\tan\beta$ cannot be too large for fixed f . As shown in Eq. (15), the correction to the Higgs VEV is proportional to $\tan^2\beta v_0^2/f^2$. If we require $\mathcal{O}(v_0^4/f^4)/\mathcal{O}(v_0^2/f^2) < 0.1$ in the expansion of v , the value of $\tan\beta$ should be below 20 (28) for $f = 4$ TeV (5.6 TeV). For a larger f , the value of $\tan\beta$ can be larger and cancel partially the suppression of v/f . Therefore, the maximal value of the cross section does not always decrease with increasing of f .

IV. FINAL STATES OF HIGGS-PAIR PRODUCTION

The Higgs-pair production can give various final states, depending on the decay modes of the Higgs boson. The SLHM corrections to the tree-level decays $h \rightarrow f\bar{f}, WW, ZZ$ are mainly from the corresponding modified couplings:

$$\Gamma(h \rightarrow XX) = \Gamma(h \rightarrow XX)_{SM} (g_{hXX}/g_{hXX}^{SM})^2, \quad (16)$$

where XX denotes WW, ZZ or fermion pairs, and $\Gamma(h \rightarrow XX)_{SM}$ is the SM decay width. g_{hXX} and g_{hXX}^{SM} are the couplings of hXX in the SLHM and SM, respectively. The couplings g_{hWW} and g_{hZZ} can be found in [12].

For the low Higgs mass, the loop-induced decay $h \rightarrow gg$ will be also important. In addition to the top quark loops, the loops of new heavy quarks (T, D, S) come into play. For another important loop-induced decay mode $h \rightarrow \gamma\gamma$, in addition to the contributions of top quark and W boson, the new charged heavy fermions (T, D, S) and gauge bosons W'^{\pm} will make contributions. Following the approach in [19], the partial decay width of $h \rightarrow \gamma\gamma$ can be calculated at one-loop level. For the SM decay channels, the relevant higher order QCD and electroweak corrections are considered using the code Hdecay [20].

In addition to the SM decay modes, the Higgs boson in the SLHM has two new important decay modes, $h \rightarrow \eta\eta$ and $h \rightarrow Z\eta$, in the kinematically allowed parameter space. Their partial widths are given by

$$\begin{aligned} \Gamma(h \rightarrow \eta\eta) &= \frac{\lambda'^2 v^2}{8\pi m_h} \sqrt{1 - x_\eta}, \\ \Gamma(h \rightarrow Z\eta) &= \frac{m_h^3}{32\pi f^2} \left(t_\beta - \frac{1}{t_\beta}\right)^2 \lambda^{3/2} \left(1, \frac{m_Z^2}{m_h^2}, \frac{m_\eta^2}{m_h^2}\right), \end{aligned} \quad (17)$$

where $x_\eta = 4m_\eta^2/m_h^2$ and $\lambda(1, x, y) = (1 - x - y)^2 - 4xy$. These two decay channels can be dominant in the allowed parameter space [12] and provide some new signatures of Higgs-pair production.

Fig. 4 shows the decay branching ratios of Higgs-pair versus the Higgs boson mass (we only plot the decay modes with branching ratio above 0.1). We see that the dominant decay channel is $hh \rightarrow WWWW$ for $150 \text{ GeV} < m_h < 200 \text{ GeV}$, similar to the SM prediction; but for Higgs mass below 140 GeV , the decay $hh \rightarrow \eta\eta\eta\eta$ will dominate over $hh \rightarrow b\bar{b}b\bar{b}$ which has the largest branching ratios in the SM. Besides, the decays $hh \rightarrow b\bar{b}\eta\eta$ and $hh \rightarrow \eta\eta WW$

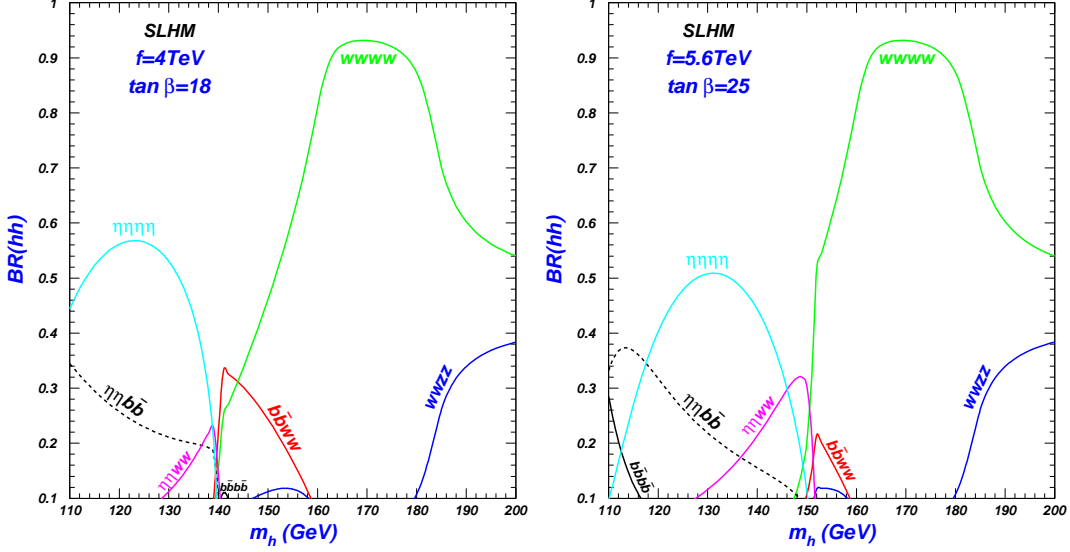


FIG. 4: The decay branching ratios of Higgs-pair as a function of the Higgs boson mass.

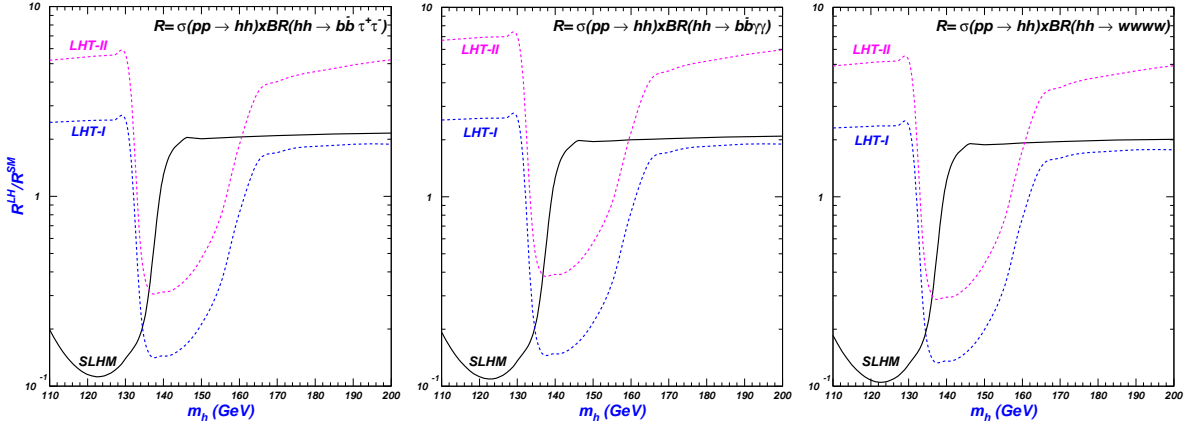


FIG. 5: The rates of $\sigma(pp \rightarrow hh) \times BR(hh \rightarrow b\bar{b}\tau^+\tau^-)$, $\sigma(pp \rightarrow hh) \times BR(hh \rightarrow b\bar{b}\gamma\gamma)$ and $\sigma(pp \rightarrow hh) \times BR(hh \rightarrow WWWW)$ in LHT-I, LHT-II and SLHM, normalized to the SM prediction. Here, $\tan\beta$ is fixed as 18 and f is taken as its lower bound, which is 4 TeV for the SLHM and 500 GeV for LHT-I and LHT-II [21].

can also be important, whose branching ratios can be much larger than the decay $hh \rightarrow b\bar{b}b\bar{b}$ in some part of the parameter space.

The decays of η have been studied in [22, 23]. For $10 \text{ GeV} < m_\eta < 100 \text{ GeV}$, η decays mainly into $b\bar{b}$, $\tau^+\tau^-$ or gg . The branching ratio of $\eta \rightarrow \tau^+\tau^-$ is about 10% of $\eta \rightarrow b\bar{b}$. With increasing of m_η , the branching ratios of $\eta \rightarrow b\bar{b}$ and $\eta \rightarrow \tau^+\tau^-$ decrease while the decay $\eta \rightarrow gg$ increases and may surpass the ratio of $\eta \rightarrow b\bar{b}$.

In the SM the promising channels are $pp \rightarrow hh \rightarrow b\bar{b}\tau^+\tau^-$ ($b\bar{b}\gamma\gamma$) for $m_h < 140 \text{ GeV}$ [24] and $pp \rightarrow hh \rightarrow WWWW$ for $150 \text{ GeV} < m_h < 200 \text{ GeV}$ [8]. In Fig. 5 we plot the

rates of $\sigma(pp \rightarrow hh) \times BR(hh \rightarrow b\bar{b}\tau^+\tau^-)$, $\sigma(pp \rightarrow hh) \times BR(hh \rightarrow b\bar{b}\gamma\gamma)$ and $\sigma(pp \rightarrow hh) \times BR(hh \rightarrow WWWW)$ normalized to the SM predictions, and compare the SLHM results with the predictions of two types of littlest Higgs models with T-parity (LHT-I and LHT-II). The detailed descriptions of LHT-I and LHT-II can be found in [3, 25]. We see that for $m_h < 130$ GeV all the three rates can be enhanced sizably in LHT-I and LHT-II, but suppressed significantly in the SLHM. For the larger value of m_h , both the SLHM and LHT-I/LHT-II can enhance sizably the SM predictions (in the SLHM for $m_h > 150$ GeV, while in the LHT for $m_h > 170$ GeV).

V. CONCLUSION

In the framework of the simplest little Higgs model (SLHM), we studied the production of a pair of neutral CP-even Higgs bosons at the LHC and obtained the following observations: (i) The Higgs-pair production rate in the SLHM can be significantly larger than the SM prediction; (ii) For a low Higgs mass the dominant decay mode of Higgs-pair is $hh \rightarrow \eta\eta\eta\eta$ (η is a CP-odd scalar) while $hh \rightarrow b\bar{b}\eta\eta$ and $hh \rightarrow \eta\eta WW$ may also have sizable ratios; (iii) For a light Higgs boson all the rates of $pp \rightarrow hh \rightarrow b\bar{b}\tau^+\tau^-$, $pp \rightarrow hh \rightarrow b\bar{b}\gamma\gamma$ and $pp \rightarrow hh \rightarrow WWWW$ can be sizably enhanced in the littlest Higgs models but severely suppressed in the SLHM; while for an intermediately heavy Higgs, all the three rates can be sizably enhanced in the littlest Higgs models and the SLHM.

Acknowledgment

We thank C. P. Yuan for discussions. This work was supported in part by the National Natural Science Foundation of China under grant Nos. 10821504, 10725526 and 10635030.

-
- [1] N. Arkani-Hamed, A. G. Cohen and H. Georgi, Phys. Lett. B **513**, 232 (2001); N. Arkani-Hamed, A. G. Cohen, E. Katz, A. E. Nelson, T. Gregoire and J. G. Wacker, JHEP **0208**, 021 (2002).
- [2] D. E. Kaplan and M. Schmaltz, JHEP **0310**, 039 (2003); I. Low, W. Skiba, and D. Smith, Phys. Rev. D **66**, 072001 (2002); S. Chang and J. G. Wacker, Phys. Rev. D **69**, 035002 (2004);

- T. Gregoire, D. R. Smith, and J. G. Wacker, Phys. Rev. D **69**, 115008 (2004); W. Skiba and J. Terning, Phys. Rev. D **68**, 075001 (2003); S. Chang, JHEP **0312**, 057 (2003); H. Cai, H.-C. Cheng, and J. Terning, JHEP **0905**, 045 (2009); A. Freitas, P. Schwaller, and D. Wyler, arXiv:0906.1816.
- [3] H. C. Cheng, I. Low, JHEP **0309**, 051 (2003); JHEP 0408, 061 (2004); H. C. Cheng, I. Low and L. T. Wang, Phys. Rev. D **74**, 055001 (2006).
- [4] N. Arkani-Hamed, A. G. Cohen, E. Katz and A. E. Nelson, JHEP **0207**, 034 (2002).
- [5] M. Schmaltz, JHEP **0408**, 056 (2004).
- [6] T. Han, H. E. Logan and L. T. Wang, JHEP **0601**, 099 (2006).
- [7] See, e.g., C. R. Chen, K. Tobe, C. P. Yuan, Phys. Lett. B **640**, 263 (2006); K. Hsieh, C. P. Yuan, Phys. Rev. D **78**, 053006 (2008); C. O. Dib, R. Rosenfeld, A. Zerwekh, JHEP **0605**, 074 (2006); L. Wang, *et al.*, Phys. Rev. D **75**, 074006 (2007); Phys. Rev. D **79**, 055013 (2009); X. F. Han, L. Wang, J. M. Yang, Phys. Rev. D **78**, 075017 (2008); arXiv:0903.5491; R. S. Hundi, B. Mukhopadhyaya, A. Nyffeler, Phys. Lett. B **649**, 280 (2007); X. Wang, Y. Zhang, H. Jin, Y. Xi, Nucl. Phys. B **810**, 226 (2009); Nucl. Phys. B **807**, 210 (2009); C.-X. Yue, H.-D. Yang, W. Ma, Nucl. Phys. B **818**, 1 (2009); H. S. Hou, Phys. Rev. D **75**, 094010 (2007); P. kai, *et al.*, Phys. Rev. D **76**, 015012 (2007).
- [8] U. Baur, T. Plehn, and D. Rainwater, Phys. Rev. Lett. **89**, 151801 (2002); Phys. Rev. D **67**, 033003 (2003).
- [9] T. Plehn, M. Spira, and P. M. Zerwas, Nucl. Phys. B **479**, 46 (1996); J. Yi *et al.*, J. Phys. G **23**, 385 (1997); J. Phys. G **23**, 1151 (1997); S. Dawson, S. Dittmaier, and M. Spira, Phys. Rev. D **58**, 40 (1998); E. W. N. Glover and J. J. van der Bij, Nucl. Phys. B **309**, 282 (1988); A. Krause, T. Plehn, M. Spira, and P. M. Zerwas, Nucl. Phys. B **519**, 85 (1998); A. A. Bendezu and B. A. Kniehl, Phys. Rev. D **64**, 035006 (2001); W. Ma, C.-X. Yue, and Y.-Z. Wang, Phys. Rev. D **79**, 095010 (2009); H. de Sandes and R. Rosenfeld, Phys. Lett. B **659**, 323 (2008); A. Arhrib, *et al.*, JHEP **0908**, 035 (2009); S. Kanemura and K. Tsumura, Eur. Phys. Jour. C **63**, 11 (2009).
- [10] J. J. Liu, *et al.*, Phys. Rev. D **70**, 015001 (2004).
- [11] L. Wang, *et al.*, Phys. Rev. D **76**, 017702 (2007); Phys. Rev. D **77**, 015020 (2008);
- [12] K. Cheung and J. Song, Phys. Rev. D **76**, 035007 (2007).
- [13] G. 't Hooft and M. J. G. Veltman, Nucl. Phys. B **153**, 365 (1979).

- [14] T. Hahn and M. Perez-Victoria, *Comput. Phys. Commun.* **118**, 153 (1999); T. Hahn, *Nucl. Phys. Proc. Suppl.* **135**, 333 (2004).
- [15] J. Pumplin *et al.*, *JHEP* **0602**, 032 (2006).
- [16] C. AMSLER *et al.*, *Phys. Lett. B* **667**, 1 (2008).
- [17] G. Marandella, C. Schappacher and A. Strumia, *Phys. Rev. D* **72**, 035014 (2005).
- [18] A. G. Dias, C. A. de S. Pires, P. S. Rodrigues da Silva, *Phys. Rev. D* **77**, 055001 (2008).
- [19] T. Han, H. E. Logan, B. McElrath and L.-T. Wang, *Phys. Lett. B* **563**, 191 (2003); Erratum-*ibid.* **603**, 257 (2004).
- [20] A. Djouadj, J. Kalinowski and M. Spira, *Computl. Phys. Commun.* **108**, 56 (2006).
- [21] J. Hubisz, P. Meade, A. Noble, M. Perelstein, *JHEP* **0601**, 135 (2006).
- [22] W. Kilian, D. Rainwater and J. Reuter, *Phys. Rev. D* **71**, 015008 (2005).
- [23] K. Cheung, J. Song, P. Tseng and Q.-S. Yan, *Phys. Rev. D* **78**, 055015 (2008).
- [24] U. Baur, T. Plehn and D. L. Rainwater, *Phys. Rev. D* **68**, 033001 (2003); *Phys. Rev. D* **69**, 053004 (2004).
- [25] See, e.g., J. Hubisz and P. Meade, *Phys. Rev. D* **71**, 035016 (2005); M. Blanke, *JHEP* **0701**, 066 (2007).